Title: Hybrid aerogel preparations as drug delivery matrices for low water-solubility drugs

Author: Peter Veres Ana M. López-Periago István Lázár Javier Saurina Concepción Domingo

PII: S0378-5173(15)30313-6
DOI: http://dx.doi.org/doi:10.1016/j.ijpharm.2015.10.045
Reference: IJP 15300

To appear in: *International Journal of Pharmaceutics*

Received date: 20-7-2015
Revised date: 28-9-2015
Accepted date: 14-10-2015

Please cite this article as: Veres, Peter, López-Periago, Ana M., Lázár, István, Saurina, Javier, Domingo, Concepción, Hybrid aerogel preparations as drug delivery matrices for low water-solubility drugs.International Journal of Pharmaceutics http://dx.doi.org/10.1016/j.ijpharm.2015.10.045

Hybrid aerogel preparations as drug delivery matrices for low water-solubility drugs

Peter Veresa,b, Ana M. López-Periagob, István Lázára, Javier Saurinac, Concepción Domingob,*

a Department of Inorganic and Analytical Chemistry, University of Debrecen, Egyetem tér 1, 4032 Debrecen, Hungary

b Institut de Ciència de Materials de Barcelona (CSIC), Campus de la UAB, 08193 Bellaterra, Spain

c Department of Analytical Chemistry, University of Barcelona, Martí i Franquès 1-11, 08028 Barcelona, Spain

*Corresponding author: Prof. Concepción Domingo, email address: conchi@icmab.es, tel.: +34935801853, fax: +34935805729

Graphical abstract

Designed hybrid aerogels (silica & gelatin) for immediate and sustained release of hydrophobic acid drugs.

Abstract

A comprehensive study of 14 hybrid aerogels of different composition with applications in drug delivery has been carried out. The overall objective was to modulate the release behavior of drug-impregnated aerogels, from an almost instantaneous release to a semi-retarded delivery prolonged during

several hours, through internal surface functionalization. The designed hybrid aerogels were composed of silica and gelatin and functionalized with either phenyl, long (16) hydrocarbon chain or methyl moiety. As model systems, three class II active agents (pKa < 5.5), ibuprofen, ketoprofen and triflusal, were chosen to impregnate the aerogels. The work relied on the use of supercritical fluid technology for both the synthesis and functionalization of the hybrid aerogels, as well as for the impregnation with an active agent using supercritical CO2 as a solvent. For the impregnated aerogels, in vitro release profiles were recorded under gastric and intestinal pH-conditions using HPLC techniques. The release behavior observed for the three studied drugs was explained considering the measured dissolution profiles of the crystalline drugs, the aerogel composition and its functionalization. Such features are considered of great interest to tailor the bioavailability of drugs with low water solubility.

Key words: supercritical CO2, hybrid aerogel, silica, gelatin, acid drugs

1. Introduction

Silica aerogel based systems constitute an emerging and promising platform for drug delivery applications, principally due to their high drug loading capacity, their capability to increase the bioavailability of hydrophobic drugs and even to improve drugs stability (Pierre and Pajonk, 2002; Smirnova et al., 2004; Ulker and Erkey, 2014; Agostini et al., 2015; Malode et al., 2015). Functionalization, hybridization and coating methods have been developed to protect silica aerogels for long term use, importantly, to avoid pore collapse in a wet environment (Soleimani-Dorcheh and Abassi, 2008; Murillo-Cremaes et al., 2014). In the pharmaceutical field, the preparation of porous organic and hybrid aerogels has increased their performance in applications related to controlled release (García-González et al., 2011), thus becoming a clear alternative to polymers as drug delivery vehicles. In this scenario, the overall

objective of this research was to design hybrid and surface functionalized aerogels, with the ability of tailoring the drug release behavior from an almost instantaneous release to a semi-retarded delivery prolonged during several hours.

Hybrid composite materials are always attractive, since they can combine diverse physicochemical characteristics in one entity (Hoffmann et al., 2006). For aerogels, coupling the high surface area of inorganic mesoporous silica with the biodegradable nature of organic constituents has led to high performance novel materials (Molvinger et al., 2004; Ramadan et al., 2010). For biomedical applications, natural biocompatible polymers are promising candidates as organic constituents. These biopolymers (e.g. proteins, polysaccharides) are, in their majority, biodegradable, available in large amounts and relatively cheap (Babu et al., 2013). Usually, they possess hydroxyl or amine groups capable of establishing inter- and intra-molecular hydrogen bonds. Due to the existence of these groups, such polymers interact strongly with water and have the capacity to form hydrogels (Oh et al., 2009; Tsioptsias et al., 2011). However, they have almost not been explored to obtain hybrid silica aerogels, and only the system chitosan/silica has been recently described (Ayers and Hunt, 2001; Molvinger et al., 2004). In this work, gelatin is used as the organic component to form hybrid silica aerogels following a sol-gel procedure and supercritical alcogel drying. Gelatin is a biopolymer derived from the hydrolysis of collagen obtained from various animal by-products. This polymer has been used as a delivery vehicle for the release of bioactive molecules and in the generation of scaffolds for tissue engineering applications (Frydrych et al., 2011; Aristippos, 2002).

The modification of the internal surface of mesoporous aerogels with specific functional groups influences the adsorption capacity and/or alters the release properties of the matrix (López-Aranguren et al., 2012; Alnaief and Smirnova, 2010; Builes et al., 2012). Hence, in this research surface modification by hydrophobic functionalization was further explored to modulate hybrid aerogel characteristics. The two different strategies used for this purpose were in situ co-condensation during silica hydrolysis with hydrophobic moieties (phenyl or C16 hydrocarbon chain) and post-gelation derivatization with

hydrophobic silanes. Hydrophobic functionalization is applied not only to alter the aerogel surface charge and reactivity (García-González et al., 2009), but often to enhance aerogel stability in wet environments (Rao et al., 2005).

In an effective drug delivery protocol, drug dissolution is the prerequisite for drug absorption in the body to get the subsequent clinical response, especially for drugs administered orally. However, around 70 % of the drugs in the R&D pipeline fit into class II in the Biopharmaceutics Classification System (BCS), presenting low solubility and low oral bioavailability (Huang and Brazel, 2001; Acharya and Park, 2006). For those active agents, if administered in the crystalline form, drug absorption is often rate limited by in vivo drug dissolution. Poorly water soluble drugs tend to be eliminated from the gastrointestinal tract before they get the opportunity to be fully dissolved and absorbed into the blood circulation system. Dose augmentation would be necessary to ensure that the drug attains the therapeutic concentration range in blood although it can cause toxicity and side effects. Introducing upgraded or advanced formulations is the approach to enhance biodisponibility for these drugs. Physical modifications, such as particle size reduction of amorphous synthesis, often aim to increase the surface area, solubility and wettability of the drug particles. Different proposed strategies are those based on the formulation of solid mixtures or matrix dispersions (Rasenack and Müller, 2004; Kerc et al., 1999; Elvira et al., 2004). Poorly water soluble crystalline drugs are preferentially formulated as molecular dispersions in porous matrices. In these conditions, drug biodisponibility is increased because no energy is required to break up the crystal lattice during dissolution. Moreover, matrix systems with a more retarded profile can be used to maintain the therapeutic dosage for a long period of time, thus, reducing the necessity of frequent dosage and increasing patient compliance.

Due to the highly porous structure of hybrid aerogels, they have been proposed as carrier matrixes for the molecular dispersion of poorly water-soluble drugs (Smirnova et al., 2004; Ulker and Erkey, 2014, García-González et al., 2011; Alnaief and Smirnova, 2010). In this study, drugs chosen for analysis are class II weak acids, namely ibuprofen (Ibu), ketoprofen (Ket), and triflusal (Trf). These active agents were used to characterize the drug delivery

capabilities of the synthesized aerogels. Triflusal is an irreversible inhibitor of the enzyme cyclo-oxygenase and it is commonly used as a platelet anti-aggregant preventer for the treatment of thrombosis diseases. Ibuprofen and ketoprofen are propionic acid derivatives belonging to the nonsteroidal anti-inflammatory drugs family with analgesic and antipyretic effects.

The unique properties of scCO2 have been advantageously exploited to prepare molecular dispersions of poorly water-soluble drug substances into porous matrices, since a high solubility of low molecular weight hydrophobic compounds in scCO2 is, usually, found (Martín and Cocero, 2008; Yasuji et al., 2008). The benefit of using scCO2 as the impregnation medium to fabricate host–guest systems has been previously demonstrated on polymeric (Kikic and Vecchione, 2003; Uzer et al., 2006; López-Periago et al., 2008) and inorganic matrices (Cooper, 2003; García-Carmona et al., 2002; Shin et al., 2000; López-Aranguren et al., 2013; López-Periago et al., 2010). The avoidance or little use of organic solvents, the intrinsic sterility of scCO2 and the fact that the final product is in a dry form and is produced in confined autoclaves are also of particular interest for pharmaceutical products manufacturing (Schutz, 2007). The objective of this study was, therefore, the use of a generic supercritical fluid technology for the synthesis and drug impregnation of hybrid aerogels. For the aerogels synthesized, functionalized and impregnated in this work, two processing characteristics of the supercritical fluid technology make the method significantly more efficient than when applying other more conventional liquid solvents. First, the null surface tension of a supercritical fluid allows the drying of alcogels preserving their porosity to form aerogels (Wagh et al., 1999; Yoda and Ohshima, 1999). Second, due to the low viscosity and high diffusivity of fluids under supercritical conditions, scCO2 solutions have the ability to penetrate and efficiently impregnate porous matrices with organic solutes, in this work selected model drugs, again without damaging the porous structure (Domingo et al., 1998; Murillo-Cremaes et al., 2010).

The quantification of the amount of drug entrapped and the characterization of the release profiles were carried out by high performance liquid chromatography (HPLC) in aqueous media at pHs 6.7 and 2.0. The use of hydrophilic aerogels resulted in either a fast or semi-retarded release as a function

of pH. Contrarily, the functionalization of the aerogels with hydrophobic moieties resulted in more prolonged release lasting several hours at both studied pHs.

2. Materials and methods

2.1 Materials

Tetramethylorthosilicate (TMOS) and gelatin, the components of the hybrid aerogels, were obtained from Fluka and Dr. Oetker, respectively. Methanol and acetone were used as the solvents for aerogel synthesis and ammonium carbonate ((NH4)2CO3) was added as a pH controller, all from Fluka. The aerogel surface modifying agents were hexadecyltrimethoxysilane (C16-TMOS), phenyltrimethoxysilane (Ph-TMOS) and hexamethyldisilazane (HMDS), all of them supplied by Sigma-Aldrich. 2-(4-(2-methylpropyl)phenyl)propanoic acid (Ibu) and 2-(3-benzoylphenyl)propanoic acid (Ket) were purchased from Sigma Aldrich, while 2-acetyloxy-4-trifluoromethyl benzoic acid (Trf) and its main metabolite 2-hydroxy-4-trifluoromethyl benzoic acid (HTB) were kindly donated by Uriach S.A. The molecular structure of modifying agents and used drugs is shown in Fig. 1a and b, respectively. CO2 (99.995 %, Carburos Metalicos S.A.) was used as the processing solvent. Milli-Q water (Millipore), formic acid (99% w/w, Merck) and methanol (HPLC grade, Panreac) were used for the preparation of the mobile phase for the chromatographic method.

2.2 Methods

2.2.1 Aerogel synthesis

Hybrid alcogels were prepared by a sol-gel procedure using different organic/inorganic phase percentage. Reagents weight used to synthesize the different studied aerogels are shown in Table 1. In a typical procedure, a given quantity of solid gelatin was first dissolved in hot water, then the solution was cooled to room temperature before adding the corresponding amount of (NH4)2CO3. A viscous solution was obtained by applying vigorous stirring, to which TMOS dissolved in methanol was added. In selected experiments, a weighted amount of either Ph-TMOS or C16-TMOS functionalizing agent was added at this point in a fraction of ca. 10, 20 and 30 v/v% with respect to TMOS. After several minutes of stirring, TMOS hydrolysis and condensation

106 produced a single phase mixture, which was poured in plastic containers to allow gelation to develop for a period of 24 h. Samples were next placed into
107 perforated aluminium containers and a multiple step solvent exchange protocol was carried out consisting on: first, samples were soaked in methanol for 24
108 h to remove water; second, methanol was replaced by acetone in two 24-h soaking steps; and finally, the acetone was extracted with scCO2 at 14 MPa and
109 80 ºC (Lázár et al., 2015). Most likely, some of the added gelatin is eliminated from the system dissolved in the aqueous phase during the multiple steps
110 solvent exchange procedure needed to dry the aerogels. For post-silanized samples, the HDMS reagent was added after the first soaking step with
111 methanol, and the system alcogel/HDMS was additionally aged during 48 h. Monolithic pieces of a dry aerogel were obtained in all cases, which were
112 further mechanically micronized to obtain a powder.

113 2.2.2 scCO2 impregnation procedure

114 The drug loading process in scCO2 was performed in a high pressure equipment described elsewhere (Murillo Cremaes et al., 2013). Experiments
115 were carried out in the batch mode. In a typical run, the autoclave (100 mL) was charged with powdered aerogel wrapped in a cylinder made of 0.45 µm
116 pore filter paper. An excess of drug (Ibu, Ket or Trf) was added at the bottom of the reactor, thus ensuring saturation of the scCO2 phase. Following this
117 experimental design, matrix and drug maintained a physical separation into the autoclave. The reactor was then filled with liquid CO2 and heated up to 45
118 ºC. The system pressure was increased to 12 MPa for the highly soluble Trf and to 20 MPa for Ibu and Ket. The autoclave was magnetically stirred at 100
119 rpm for a period of 6 h, after which the reactor was depressurized and the loaded aerogel was recovered. The depressurization rate was 0.2-0.3 MPa min-1
120 to avoid drug crystallization.

121 2.3 Characterization

122 2.3.1 Solid characterization

The thermal behavior of hybrid aerogels and the quantification of the loaded modifiers and drugs were assessed by thermogravimetric analysis (TGA) using a Perkin Elmer 7 TGA instrument. Thermal transitions were studied by differential scanning calorimetry (DSC) with a Mettler Toledo 822e/400 instrument. Both kinds of measurements were carried out under N2 atmosphere at a 10 ºC min−1 heating rate. The crystallinity of the loaded drugs was analyzed by X-ray powder diffraction (XRD) using a Rigaku Rotaflex RU-200 B spectrometer. Textural characteristics of bare and impregnated matrices were studied by low-temperature N2 adsorption–desorption analysis (ASAP 2000 Micromeritics Inc.). Prior to measurements, samples were dried under reduced pressure (<1 mPa) at 80 ºC for 24 h. Specific surface area (as) was determined by the BET method. The volume (Pv) was determined from the N2 adsorption isotherm using the BJH method.

2.3.2 HPLC characterization

The liquid chromatograph equipment consisted of an Agilent 1100 series instrument furnished with a G1311 quaternary pump, a G1379A degasser, a G1392A autosampler and a G1315B diode array spectrophotometric detector. Instrumental control and data acquisition and treatment were carried out with a PC using the Agilent Chemstation software. The analytical column was a Synergy Hydro-RP C18 (150 mm×4.6 mm i.d., particle size 4 µm) from Phenomenex. Analytes were eluted isocratically using 0.1 v/v% formic acid aqueous solution and methanol. The percentage of methanol in the eluent was 80 v/v% for Trf/HTB and Ket, and 90 v/v% for Ibu. The mobile phase flow rate was 1 mL min-1 and the injection volume was 10 µL. Trf/HTB, Ket and Ibu were detected at 280, 254 and 220 nm, respectively. A complete description of the procedure can be found in (Argemí et al., 2008). This procedure was used in the determination of the percentage of impregnation and in the monitoring of the drug release.

HPLC methods were first applied to quantify the overall amount of drug loaded in the different aerogel samples. The percentage was determined after soaking a weighed sample amount (~ 5-10 mg) in 10 mL of methanol. 10 µL of the resulting solutions were injected in the column of the

chromatographic system. In the case of Trf/HTB systems, concentrations of both drug and metabolite were quantified and data presented in this work corresponded to the sum of both values, expressed as the total triflusal (Trf(T)).

HPLC analysis was also used to follow the kinetics of drug dissolution for pristine drugs and of drug release for selected aerogel samples. The drug delivery profiles were evaluated in both 10 mM HCl (pH 2.0) and 50 mM hydrogenphosphate / dihidrogenphosphate buffer (pH 6.7) aqueous solutions, thus, simulating gastric and intestinal pH-condition, respectively. In these experiments, a weighed sample (~ 5-7 mg) was added to 25 mL of preheated (37 +/- 0.5 °C) buffer solution. The stirring rate and temperature were fixed at 60 rpm and 37 ºC, respectively. For each measurement, 250 µL buffer was recovered, and 10 µL were injected into the column. Assays were performed in triplicate that allowed the release profiles and variability ranges to be established.

3. Results and discussion

3.1 Aerogels composition

Four different gelatin:silica precursor weight ratios, between 3 and 30 wt%, were added to the reactor to synthesize the hybrid aerogels (Table 1). In particular, ratios of 3, 10, 20 and 30 wt% were used to synthesize samples referred as H3, H10, H20 and H30, respectively. The gelatin mass incorporated in these hybrid aerogels after processing was estimated by TGA from the weight loss in the range 300-500 ºC (Fig. 2a). In this temperature interval, some condensation of vicinal -OH groups could also take place in the inorganic silica phase. However, the lost of weight in this range due to the lost of water molecules expelled by the inorganic phase is below 1 wt% and has was considered negligible (Murillo-Cremaes et al., 2013). The TGA estimated weight percentage of gelatin in hybrid aerogels is given in Table 2. This ratio was from ca. 3 to 24 wt% in samples with the lowest (H3) and the highest amount of added gelatin (H30).

The gelatin/silica aerogels are hydrophilic porous materials. To obtain products with different characteristics and applications, the hybrid aerogels were further modified by functionalization on the surface. Two different functionalization approaches were evaluated, applied either during the sol-gel process or after gelation. In the first method, aerogels with a low percentage of gelatin (H3), were modified during the sol-gel reaction by co-condensation of TMOS and either Ph-TMOS (sample H3_Ph) or C16-TMOS (sample H3_C16) added in a ratio of TMOS:functionalizing agent of 90:10, 80:20 or 70:30 v/v% (Table 1). For the two studied TMOS additives, a hydrophobic group was incorporated into the silica matrix via a hydrolytically stable Si-C covalent bond (≡O-Si-Ph or ≡O-Si-C16H33) (Wei et al., 2004; Hegde and Rao, 2006). In the second tactic, the hybrid gel was post-functionalized after aging, but before drying, by adding HMDS, a difunctional trimethylsilyl silane that is known to be highly reactive with surface silanols, giving ammonia as a side product (Rao et al., 2004). In this case, the hydrogen in the surface silanol groups is replaced by the hydrolytically stable ≡O-Si-(CH3)3 group (Kartal and Erkey, 2010). Following

this procedure, hybrid aerogels with different silica:gelatin ratios were derivatized by adding an excess of the silylation component, in a weight percentage close to 50 wt% with respect to the added weight of aerogel TMOS and gelatin components.

TGA was used to estimate the final composition of the functionalized aerogels. Gelatin decomposition was previously established to occur between 300 and 500 ºC (Fig. 2a). The degradation temperature of modifiers used depends on the chemical structure of the grafted molecules. Fig. 2b shows the TGA profiles corresponding to H3 aerogels treated with each one of the studied modifiers. For Ph-TMOS and HMDS treated aerogels, the hydrolytically stable ≡Si-C covalent bond in the ≡Si-Ph and ≡Si-(CH3)3 layers remained intact up to 550 ºC. As a consequence, for these samples the weight loss occurred in two uneven stages: the first one corresponded to gelatin degradation (300-500 ºC) and the second resulted from the Si-C cleavage occurring in the 550-700 ºC temperature interval. From the TGA weight loss in the second temperature interval, it could be estimated that aerogel samples were modified with ca. 4-9 and 5-6 wt% of -Ph and -(CH3)3 organic moieties, respectively (Table 2). In contrast, for the aerogel modified with -C16 (H3_C16 samples) the grafted hydrocarbon chain starts to decompose by cleavage of C–C bonds at ca. 250-300 ºC and continue up to 700 ºC, temperature interval in which the Si-C bond is broken. Therefore, the weight loss of gelatin and modifier were overlapped. Assuming a gelatin loss of weight of ca. 4 wt% in the H3 type samples, the estimated amount of C16 modifier incorporated to the sample was ca. of 2-6 wt% (Table 2).

The grafted modifiers have remarkably different molecular weight values (Mw), namely: 77, 225 and 45 g mol-1 for -C6H5 (Ph), -C16H33 (C16) and -(CH3)3 (HMDS), respectively, which would result in different surface molecular densities for similar weight percentages of incorporated product. To facilitate comparison, molecular surface densities (Sρ) were calculated by using the BET values of the specific surface area of the raw matrices (as [nm2 g-1]) and the TGA measured amount of deposited modifier (ds [g(modifier) g-1] (Table 2). Surface grafting density was calculated using the formula:

$$\frac{d_s \cdot 6 \cdot 10^{23}}{M_w \cdot a_s} = S\rho\ [\text{molecule nm}^{-2}]$$

Relatively high density values of 1.0-1.7 molecule nm-2 were estimated for the silanized products, and of 0.5-1.0 molecule nm2 for -Ph treated aerogels. On the contrary, aerogels functionalized with the long carbon chain -C16 had surface grafting density values of only 0.1-0.2 molecule nm2.

3.2 Microstructure and textural properties of aerogels

The microstructure of the prepared composite aerogels was studied in regard of their morphology and textural properties. Pictures of sample H20, with a fairly high gelatin content (18 wt%), are shown in the SEM pictures of Fig. 3. Only the microstructure typical of silica aerogel can be observed in the images. No separate polymer phase was visible in any portion of the sample, thus indicating that the two phases were intimately mixed at this scale. The measured percentages of gelatin in the hybrid aerogels (Table 2) were similar to the added amounts (Table 1), suggesting the full incorporation of this phase to the silica primary particles. Sol-gel nanocomposites were formed as colloidal hybrid sol particles, which subsequently aggregated to gels and resulted in aerogels after drying (Watzke and Dieschbourg, 1994).

Silica aerogels possess a wide variety of extraordinary properties, including very high porosity (95-99 %) and pore volume (2.5-3 cm3 g-1), high specific surface area (700-1500 m^2 g-1) and mesoporosity. Often, hybrid aerogels have lower values of textural properties than pristine silica, but still they are obtained as highly porous materials in the mesopore range. The N2 adsorption/desorption isotherms recorded for the hybrid aerogels synthesized with different gelatin dosages had a type IV profile (IUPAC classification), characteristic of mesoporous materials, including also macropores. Table 2 reports the textural data for hydrophilic H3-H30 hybrid aerogels. For sample H3, with the lowest gelatin content, the surface area and pore volume were ca. 700 m2 g-1 and 2.1 cm3 g-1. By increasing the percentage of gelatin in the sample, these values decreased to ca. 300 m2 g-1 and 1.2 cm3 g-1 in H30, but still maintained the mesoporous characteristics and the high surface area values. Irrespective of the aerogel composition, the mean pore diameter value was in the order of

198 magnitude of 15 nm. Finally, functionalization of the aerogels surface by co-condensation (H3) or silane derivatization (H3 and H20) did not have a significant
199 influence in the measured values of both the specific surface area and pore volume when compared to non-functionalized similar aerogels (Table 2).

200 In the N2 adsorption measurements, the intensity of the interaction of the adsorbate with the surface of the adsorbent can be assessed from the C
201 constant of the BET equation (Sing, 1998). Although rigorous interpretation of the C parameter, combined with its use for the determination of surface
202 energies, has fundamental limitations, this simplistic qualitative approach gives an idea of the hydrophobic/hydrophilic degree of the adsorbent surface: the
203 lower the C constant value, the lower the hydrophilicity. Pure silica aerogels have values of C of ca. 100. As it can be observed in Table 2, hybrid H3-H30
204 aerogels prepared in this work presented values of C in the order of 80, independently of the gelatin content, indicating hydrophilic compounds. The C values
205 for the -Ph modified aerogels (H3_Ph) and silylated samples (H3_sil, H20_sil) were reduced to ca. 30-50, pointing towards a decrease of the aerogel surface
206 polarity, which is the result of the presence of the hydrophobic functionalizing agent. In contrast, C values measured for the -C16 modified aerogel (H3_C16)
207 were similar to those corresponding to the pristine hybrid matrix H3, likely reflecting the low surface grafting density values estimated for this modifier (0.1-
208 0.2 molecule nm-2), not enough to significantly modify the thermodynamic properties of the aerogel surface.

209 3.3 Impregnated aerogels

210 The hybrid aerogel systems described previously were impregnated with Ibu, Ket or Trf by using scCO2 as a solvent. The high hydrophobicity of
211 these drugs makes them soluble in scCO2 at 35-45 °C and pressures above 90 bar. The solubility of ibuprofen in scCO2 was found to be in the order of
212 4x10−3 mole fraction at 20 MPa and 35 ºC (Charoenchaitrakool et al., 2000). Under similar conditions, the solubility of ketoprofen was reduced to a value of
213 8x10-5 mole fraction (Macnaughton et al., 1996). The lower solubility value found for ketoprofen with respect to ibuprofen was linked to the high molecular
214 weight of the former. For triflusal, the presence of the hydrophobic trifluoromethyl group renders a pronounced effect in the interaction of Trf molecules
215 with scCO2 enhancing the solubility to values of 3×10−2 mole fraction at 35 ºC and 20 MPa (López-Periago et al., 2009).

After scCO2 impregnation, the first estimation of drug loading values was performed by TGA. Illustrative TGA profiles, corresponding to aerogel H3 loaded with any of the three studied drugs (e.g. Ibu@H3, Ket@H3 and Trf(T)@H3), are shown in Fig. 4a. Impregnation values were roughly calculated from the weight loss in the interval 150-550 ºC, after subtracting the fraction corresponding to the matrix (gelatin) weight loss (ca. 4 wt%). Following the described scCO2 impregnation procedure, high loading values were found, in the order of 19, 13 and 27 wt% for Ibu@H3, Ket@H3 and Trf(T)@H3 samples, respectively. These loadings are considered as particularly high for systems in which the drug is not deposited in the form of either crystalline or amorphous particles. Higher drug loading values have been reported, but involving the formation of crystals inside of the aerogel pores (Rajanna et al. 2015, Gorle et al. 2008). In order to confirm the loading percentages, more accurate determination relying on HPLC analysis from three independent replicates was conducted. Results given in Table 2 are those obtained from HPLC measurements. Note that for impregnated H3 samples, loading values estimated by either TGA or HPLC were similar. The highest loading values were obtained for Trf(T) drug (ca. 25-29 wt%), followed by Ibu (ca. 19-24 wt%) and Ket with the lowest loading values (ca. 11-15 wt%).

XRD was used to assess the occurrence or the absence of a crystalline arrangement for the impregnated drugs. Spectra were recorded in the 2θ range of 5-35º and for low gelatin content matrices H3 they are shown in Fig. 4b. The three studied drugs could be readily identified in this range by their most intense peaks (Fig. 4b). For the three studied drugs loaded into H3 aerogels, spectra showed only a broad band centered at ca. 22º, which was typical of amorphous silica. Diffraction peaks corresponding to Trf, Ibu or Ket crystalline forms were not detected in the XRD patterns of the composite products. This result indicates the absence of drug crystallization inside of the aerogel pores after supercritical impregnation. Complementarily, DSC analysis (not shown) was used to further confirm the absence of drug crystals or amorphous forms in these products. Within the studied DSC temperature interval (up to 450 ºC), thermal transitions were inexistent for the studied H3 matrices, as well as for this matrix loaded with the different drugs. Unsupported drugs melt

233 in the 80-120 ºC temperature interval exhibiting a sharp endothermic peak in the DSC spectra. Hence, XRD and DSC results suggested that the drug was
234 most likely dispersed inside the matrices at a molecular level, rather than in the crystalline or amorphous solid form (Kazarian and Martirosyan, 2002; López-
235 Periago et al., 2009). In fact, to generate crystalline particles inside of the pores a sudden change in solubility, created, for instance, by fast pressure release,
236 has been described as necessary (Gorle et al., 2010).

237 Synthesized hybrid aerogel are highly hydrophilic, having a high number of surface -OH and -NH groups. These reactive surface moieties may be able
238 to form hydrogen bond with the carboxylic acid groups of studied drug molecules, which favored the molecular dispersion and stabilized thermally the drugs
239 against degradation, since TGA analysis showed that they were stable up to temperatures of 300 ºC and higher (Fig. 4a). For these samples, the textural
240 properties were also modified after drug impregnation, resulting in a reduction of the specific surface area and pore volume to values of ca. 400-450 m2 g-1
241 and 1.5-1.6 cm3 g-1, respectively, which likely account for the space occupied by the drug molecules. Moreover, the given C values were in the order of 30-
242 40 for H3 impregnated matrices, which were in the range of approximately half of the value of the raw H3 aerogel (Table 2), indicating surface
243 hydrophobization by drug impregnation.

244 The influence of aerogel functionalization on drug loading was further studied by HPLC (Table 2). For hydrophilic matrices, constituted exclusively by
245 silica and gelatin, the gelatin percentage did not have any significant influence on drugs uptake at the studied silica:gelatin ratios (Fig. 5a). The effect on the
246 drug uptake when modifying the aerogel with the -Ph (Fig. 5b) or -C16 (Fig. 5c) hydrophobic agent was found to be negligible for any of the three drugs
247 studied. For these systems, impregnated values were in the order of 18-27, 7-18, 19-29 wt% for Ibu, Ket and Trf(T), respectively (Table 2). For the -C16
248 modified aerogels, this result can be attributed to the low attained surface grafting density, but it was surprising for the -Ph modified products. Contrarily,
249 formation of hydrophobic gelatin-silica aerogels by exposition to hexamethyldisilazane and further drug impregnation resulted, in general, in materials with

a lower amount of adsorbed drugs than the raw matrices (Fig. 5d). Loading differences were more significant for Ibu and Ket drugs than for Trf(T). The decrease in the uptake can be related to the reduction of the drug adsorption sites already occupied by silyl moieties.

3.4 Drug dissolution and release profiles

Drug dissolution profiles of pristine drugs and loaded aerogel systems were monitored in vitro according to the HPLC methodology described in section 2.3. Assays were carried out in two dissolution media, biorelevant and widely applied to similar studies, with a pH of either 6.7 (intestinal pH) or 2.0 (gastric pH). A preliminary dissolution test was carried out for each pristine drug under similar pH conditions (Fig. 6). Crystalline drugs were rapidly dissolved in the first few minutes, either totally (basic pH) or up to saturation values (acid pH). This is the common behavior expected for the studied acidic drugs, with pKa values of 4.40, 4.76 and 4.15 for Ibu, Ket and Trf, respectively (Sheng et al., 2009). Performed measurements gave an estimation of drugs solubility under studied experimental conditions: at pH 2 and 37 ºC, measured solubility values were in the order of 0.06, 0.26 and 0.69 mg mL-1 for Ibu, Ket and Trf(T), respectively, while at pH 6.7 and 37 ºC, the solubility of the three compounds was higher than 0.7 mg mL-1, which was the highest value assayed. The observed increase in dissolution at pH 6.7, particularly evident for Ibu and Ket active agents (Fig. 6a,b), was related to an enhanced driving force for the forward reaction between the weakly acid drug and the basic species in the medium. The Trf behavior was more complex (Fig. 6c), since aside from solubility issues, this molecule is unstable at neutral and alkaline pH (Ferrit et al., 2008) undergoing a progressive decomposition to HTB (Argemí et al., 2008). The metabolite HTB is also highly active as a platelet aggregation inhibitor, hence, its degradation does not represent a remarkable shortcoming from a pharmaceutical point of view. However, analytically this decomposition makes more difficult the evaluation of the behavior of the drug in aqueous media.

The drug release profiles were studied for samples involving either a hydrophilic (H3) or hydrophobic (H3_sil) matrix. Drug release profiles from the hydrophilic H3 matrix are shown in Fig. 7. At pH 6.7, drug dissolution for the three studied active agents occurred almost instantaneously (Fig. 7a-c). On the

contrary semi-retarded release profiles were recorded at pH 2.0. For Ibu at pH 2.0, a release of drug of ca. 50 % was observed in a first burst stage, followed of a slow delivery step giving ca. 70 % of drug released after 5 h of dissolution test (Fig. 7a). For Ket at pH 2.0, the initial burst release attained a value as high as 80 % and after 5 h the drug was completely released to the acid media (Fig. 7b). For Trf(T) at pH 2.0, the initial burst provided an immediate relief of 40 % of the loaded drug, reaching a value of drug dissolution of 90 % after 5 h of test (Fig. 7d). It is worth mentioning that the dissolution rate for the three studied drugs from the H3 matrix was faster in basic medium than at pH 2.0, which corresponded to the medium with the measured lowest solubility values. Hence, the observed semi-retarded release behavior under acidic conditions could not be related to drug solubility, but to the specific interaction established between the matrix and each drug as a function of pH. Analytes studied are quite apolar (the estimated logP values for Ibu, Ket and Trf are 3.7, 2.8 and 2.3, respectively) and are mainly protonated (neutral) at pH 2.0, while at pH 6.7 the deprotonated (anionic) species of all the drugs are present as the major species. The protonated species mainly occurring a pH 2.0 seems to interact more strongly with the hydroxylated matrix surface, probably through hydrogen bonds, thus, retarding drug release.

In Fig. 7c,d, the separate Trf and HTB curves are shown at the two studied pHs, together with the total triflusal drug release profiles. The percentages of Trf and HTB inside of the matrices were calculated from the corresponding chromatographic peaks at the initial stages of the release. Those values were considered to mirror the degree of hydrolysis of the encapsulated drug, and were related to the percentage of drug degradation during preparation and storage. As shown in Fig. 7c,d, the molar percentage of Trf hydrolysis to HTB in the hydrophilic aerogels was about 10 mol%. Found values were consistent with the values obtained in the instantaneous HPLC dissolution process carried out to quantify the overall amount of drug loaded in the different aerogel samples. It is noteworthy that the degree of hydrolysis was relatively low, being the Trf well preserved inside the hydrophilic aerogel

matrices. This behavior was attributed to the acidity provided to the adsorbed water by the SiO2 matrix, which in turns stabilized the Trf molecules against hydrolysis. At pH 6.7, Trf transformation to HTB continued during the dissolution test, reaching a value of almost 20 mol% after 120 min (Fig. 7c).

The role of modifiers in the silica aerogel, including gelatin in the bulk and hydrophobic agents on the surface, is analyzed by comparison with published data for pure silica aerogels having surface areas of 600-800 m2g-1 and drug loadings in the order of 10-20 wt%. For the ibuprofen@silica aerogel system, release data is published at neutral pH showing a delivery of 80 % of the drug after 30 min (Mehling et al. 2009). For the ibuprofen@H3 system studied in this work, the release of 80 % was attained after 10 min in neutral pH and retarded to more than 300 min at acid pH. For the ketoprofen@silica aerogel system, it has been shown that 60 min are necessary to release 80 % of the drug at acid pH (Smirnova et al. 2004), similar to the value found in this work for the ketoprofen@H3 system. For the TRF@silica aerogel system, previous studies showed that 80 % of the drug was released after 20 min in both acid and basic pH (Murillo-Cremaes et al. 2013). However, for the TRF@H3 samples, periods of 60 and >300 min were necessary to reach a delivery of 80 % at neutral and acid pH, respectively.

The release behavior of the hydrophobic drugs dispersed in modified hydrophobic aerogels was assessed in the matrix with the lowest gelatin content treated with HDMS (H3_sil sample). For the three studied drugs, a prolonged release over time was observed for the impregnated drug@H3_sil samples when compared to the release profiles of similar drug@H3 aerogels (Fig. 8). This behavior was observed at both of the studied pHs. The described fast release observed for the drug@H3 samples at pH 6.7 turned into a two-step release profiled in similar drug@H3_sil samples, involving an initial burst of 40, 15 and 20 % release for Ibu, Ket and Trf(T), followed of a slow delivery reaching values of 75, 35 and 80 % release for Ibu, Ket and Trf(T) after 5h (Fig. 8a,b,c). At pH 2, similar initial burst values than at pH 6.7 were noticed for drug@H3_sil samples, although a slightly slower drug release was measured at the acidic pH. At pH 2, values of only 55, 30 and 65 % release were measured for Ibu, Ket and Trf(T) after 5 h (Fig. 8a,b,d).

4. Conclusions

Facile and robust manufacturing methodologies of complex materials, with potential added value as controlled drug delivery systems, are highly sought-after in the pharmaceutical industry. In this work, we have demonstrated that supercritical fluid technology in general, and supercritical CO2 in particular, can be designed as a versatile fabrication route used to obtain highly-porous hybrid (silica:gelatin) aerogels, functionalized with diverse hydrophobic agents (phenyl, C16 or methyl) and further loaded with an active pharmaceutical ingredient. A considerable high amount of drug was loaded into the matrices (ca. 15-25, 10-15 and 20-30 wt% for Ibu, Ket and Trf(T), respectively), dispersed in a molecular form inside of the hybrid aerogels, i.e., not crystallized. For the studied class II BSC weakly acidic drugs, both immediate and semi-retarded release could be achieved based on matrix composition and surface hydrophobicity. The outcomes of this work are expected to be significant for the pharmaceutical industry, since a large amount of the active agents in the R&D pipeline fit into class II in the BCS system. These results demonstrate the possibility of tailoring the drug release profile by using complex hybrid aerogel systems.

Acknowledges

This work was partially financed by the Generalitat de Catalunya and the Spanish MEC with projects NASSOS 2014SGR377 and Superfactory CTQ2014-56324. The work was further supported by the TÁMOP-4.2.2.A-11/1/KONV-2012-0036 project co-financed by the European Union and the European Social Fund. P. Veres and A. López-Periago acknowledge the TÁMOP-4.2.4B/2-11/1-2012-0001 project and the RyC-2012-11588 contract, respectively.

317

References

Acharya, G., Park, K., 2006. Mechanisms of controlled drug release from drug-eluting stents. Adv. Drug Deliv. Rev. 58, 387-401.

Agostini, E., Winter, G., Engert, J., 2015. Water-based preparation of spider silk films as drug delivery matrices. J. Control Release 213, 134-141.

Alnaief, M., Smirnova, I., 2010. Effect of surface functionalization of silica aerogel on their adsorptive and release properties. J. Non-Cryst. Solids 356, 1644-1649.

Argemí, A., López-Periago, A., Domingo, C., Saurina, J. 2008. Spectroscopic and chromatographic characterization of triflusal delivery systems prepared by using supercritical impregnation technologies. J. Pharm. Biomed. Anal. 46, 456–462.

Aristippos, G., 2002. Soft Gelatin Capsules. Protein-Based Films and Coatings: CRC Press.

Ayers, M.R., Hunt, A.J., 2001. Synthesis and properties of chitosan–silica hybrid aerogels. J. Non-Cryst. Solids 285, 123–127.

Babu, R.P., O'Connor, K., Seeram, R., 2013. Current progress on bio-based polymers and their future trends. Progr. Biomater. 2, 1-16.

Builes, S., López-Aranguren, P., Fraile, J., Vega, L.F., Domingo, C., 2012. Alkylsilane-functionalized microporous and mesoporous materials: molecular simulation and experimental analysis of gas adsorption. J. Phys. Chem. C 116, 10150-10161.

Charoenchaitrakool, M., Dehghani, F., Foster, N.R., Chan, H.K., 2000. Micronization by rapid expansion of supercritical solutions to enhance the dissolution rates of poorly water-soluble pharmaceuticals. Ind. Eng. Chem. Res. 39, 4794-4802.

Cooper, A.I., 2003. Porous materials and supercritical fluids. Adv. Mater. 15, 1049–1059.

Domingo, C., García-Carmona, J., Llibre, J., Rodríguez-Clemente, R., 1998. Organic-guest/microporous-host composite materials obtained by diffusion from a supercritical solution. Adv. Mater. 10, 672-676.

Elvira, C., Fanovich, A., Fernández, M., Fraile, J., San Román, J., Domingo, C., 2004. Evaluation of drug delivery characteristics of microspheres of PMMA–PCL–cholesterol obtained by supercritical-CO2 impregnation and by dissolution–evaporation techniques, J. Contr. Release. 99, 231-240.

Ferrit, M., del Valle, C., Martínez, F., 2008. The influence of the structural characteristics of the substrate and the medium on the stability of triflusal and acetylsalicylic acid in micellar systems. J. Molec Liq. 142, 64-71.

339 Frydrych, M., Wan, C., Stengler, R., O'Kelly, K.U., Chen, B., 2011. Structure and mechanical properties of gelatin/sepiolite nanocomposite foams. J. Mater.
340 Chem. 21, 9103-9111.

341 García-Carmona, J., Fanovich, M.A., Llibre, J., Rodriguez-Clemente, R., Domingo, C., 2002. Processing of microporous VPI-5 molecular sieve by using
342 supercritical CO2: stability and adsorption properties. Microp. Mesop. Mater. 54, 127-137.

343 García-González, C.A., Saurina, J., Ayllón, J.A., Domingo, C., 2009. Preparation and characterization of surface silanized TiO2 nanoparticles under compressed
344 CO2: reaction kinetics. J. Phys. Chem. C 113, 13780-13786.

345 García-González, C.A., Alnaief, M., Smirnova, I., 2011 Polysaccharide-based aerogels-Promising biodegradable carriers for drug delivery systems. Carb.
346 Polym. 86, 1425-1438.

347 Gorle, B.S.K., Smirnova, I., Dragan, M., Dragan, S., Arlt,W., 2008. Crystallization under supercritical conditions in aerogels. J. Supercrit. Fluids 44, 78-84.

348 Gorle, B.S.K., Smirnova, I., Arlt, W., 2010. Adsorptive crystallization of benzoic acid in aerogels from supercritical solutions. J. Supercrit. Fluids 52, 249-257.

349 Hegde, N.D., Rao, A.V., 2006. Organic modification of TEOS based silica aerogels using hexadecyltrimethoxysilane as a hydrophobic reagent. Appl. Surf. Sci.
350 253, 1566-1572.

351 Hoffmann, F., Cornelius, M., Morell, J., Fröba, M., 2006. Silica-Based Mesoporous Organic–Inorganic Hybrid Materials. Ang. Chem. Int. Ed. 45, 3216-3251.

352 Huang, X., Brazel, C.S., 2001. On the importance and mechanisms of burst release in matrix-controlled drug delivery systems. J. Control. Release 73, 121-
353 136.

354 Kartal, A.M., Erkey, C., 2010. Surface modification of silica aerogels by hexamethyldisilazane–carbon dioxide mixtures and their phase behavior. J. Supercrit.
355 Fluids 53, 115-120.

356 Kazarian, S.G., Martirosyan, G.G., 2002. Spectroscopy of polymer/drug formulation processed with supercritical fluids: in situ ATR-IR and Raman study of
357 impregnation of ibuprofen into PVP. Int. J. Pharm. 232, 81-90.

358 Kerc, J., Srcic, S., Knez, J., Sencar-Bozic, P., 1999. Micronization of drugs using supercritical carbon dioxide. Int. J. Pharm. 182, 33-39.

359 Kikic, I., Vecchione, F., 2003. Supercritical impregnation of polymers. Current Op. Solid State Mater. Sci. 7, 399-405.

Lázár, I., Bereczki, H.F., Manó, S., Daróczi, L., Deák, G., Fábián, I., Csernátony, Z., 2015. Synthesis and study of new functionalized silica aerogel poly(methyl methacrylate) composites for biomedical use. Polym. Compos. 36, 348-358.

López-Aranguren, P., Saurina, J., Vega, L.F., Domingo, C., 2012. Sorption of tryalkoxysilane in low-cost porous silicates using a supercritical CO2 method. Microp. Mesop. Mater. 148, 15-24.

López-Aranguren, P., Vega, L.F., Domingo, C., 2013. A new method using compressed CO2 for the in situ functionalization of mesoporous silica with hyperbranched polymers. Chem. Commun. 49, 11776-11778.

López-Periago, A.M., Vega, A., Subra, P., Argemí, A., Saurina, J., García-González, C.A., Domingo, C., 2008. Supercritical CO2 processing of polymers for the production of materials with applications in tissue engineering and drug delivery. J. Mater. Sci. 43, 1939-1947.

López-Periago, A., Argemí, A., Andanson, J.M., Fernández, V., García-González, C.A., Kazarian, S.G., Saurina, J., Domingo, C., 2009. Impregnation of a biocompatible polymer aided by supercritical CO2: evaluation of drug stability and drug–matrix interactions. J. Supercrit. Fluids 48, 56-63.

López-Periago, A.M., García-González, C.A., Saurina, J., Domingo, C., 2010. Preparation of trityl cations in faujasite micropores through supercritical, CO2 impregnation. Microp. Mesop. Mater., 132, 357-362.

Macnaughton, S.J., Kikic, I., Foster, N.R., Alessi, P., Cortesi, A., Colombo, I., 1996. Solubility of anti-inflammatory drugs in supercritical carbon dioxide. J. Chem. Eng. Data 41, 1083-1086.

Malode, V.N., Paradkar, A., Devarajan, P.V., 2015. Controlled release floating multiparticulates of metoprolol succinate by hot melt extrusion. Int. J. Pharm. 491, 345-351.

Martín, A., Cocero, M.J., 2008. Micronization processes with supercritical fluids: fundamentals and mechanisms. Adv. Drug Deliv. Rev. 60, 339-350.

Mehling, T., Smirnova, I., Guenther, U., Neubert, R.H.H., 2009. Polyxaccharide-based aerogels as drug carriers. J Non-Cryst. Solids 355, 2472-2479.

Molvinger, K., Quignard, F., Brunel, D., Boissière, M., Devoisselle, J.-M., 2004. Porous chitosan-silica hybrid microspheres as a potential catalyst. Chem. Mater. 16, 3367-3372.

Murillo-Cremaes, N., López-Periago, A.M., Saurina, J., Roig, A., Domingo, C., 2010. A clean and effective supercritical carbon dioxide method for the host–guest synthesis and encapsulation of photoactive molecules in nanoporous matrices. Green Chem. 12, 2196-2204.

382 Murillo-Cremaes, N., López-Periago, A.M., Saurina, J., Roig, A., Domingo, C., 2013. Nanostructured silica-based drug delivery vehicles for hydrophobic and
383 moisture sensitive drugs. J. Supercrit. Fluids 73, 34-42.

384 Murillo-Cremaes, N., Subra-Paternault, P., Saurina, J., Roig, A., Domingo, C., 2014. Compressed antisolvent process for polymer coating of drug-loaded
385 aerogel nanoparticles and study of the release behavior. Colloid Polym. Sci. 292, 2475-2484.

386 Oh, J.K., Lee, D.I., Park, J.M., 2009. Biopolymer-based microgels/nanogels for drug delivery applications. Progr. Polym. Sci. 34, 1261-1282.

387 Pierre, C., Pajonk, G.M., 2002. Chemistry of aerogels and their applications. Chem. Rev. 102, 4243-4265.

388 Rajanna, S. K., Kumar, D., Vinjamur, M., Mukhopadhyay, M., 2015. Silica aerogel microparticles from rice husk ash for drug delivery. Ind. Eng. Chem. Res. 54,
389 949-956.

390 Ramadan, H., Coradin, T., Masse, S., El-Rassy, H., 2010. Synthesis and characterization of mesoporous hybrid silica-polyacrylamide aerogels and xerogels.
391 Silicon 3, 1-13.

392 Rao, A.V., Bhagat, S.D., Barboux, P., 2004. Comparative studies on surface chemical modification of silica aerogels based on various organosilane compounds
393 of the type RnX4-n. J. Non-Cryst. Solids 350, 216-220.

394 Rao, A.V., Kulkarni, M.M., Bhagat, S.D., 2005. Transport of liquids using superhydrophobic aerogels. J. Colloid Interface Sci. 285, 413-418.

395 Rasenack, N., Müller, B.W., 2004. Micron-size drug particles: common and novel micronization techniques. Pharm. Dev. Tech. 9, 1-13.

396 Schutz, E., 2007. Supercritical fluids and applications-a patent review. Chem. Eng. Tech. 30, 685-688.

397 Sheng, J.J., McNamara, D.P., Amidon, G.L., 2009. Toward an in vivo dissolution methodology: a comparison of phosphate and bicarbonate buffers. Molec.
398 Pharm. 6, 29-39.

399 Shin, Y., Zemanian, T.S., Fryxell, G.F., Wang, L.Q., Liu, J., 2000. Supercritical processing of size selective microporous materials. Microp. Mesop. Mater. 37,
400 49-56.

401 Sing, K.S.W., 1998. Adsorption methods for the characterization of porous materials. Adv. Colloid Interf. Sci. 76-77, 3-11.

402 Smirnova, I., Suttiruengwong, S., Arlt, W., 2004. Feasibility study of hydrophilic and hydrophobic silica aerogels as drug delivery systems. J. Non-Cryst. Solids
403 350, 54-60.

404 Soleimani-Dorcheh, A., Abbasi, M.H., 2008. Silica aerogel; synthesis, properties and characterization. J. Mater. Proc. Tech. 199, 10-26.

405 Tsioptsias, C., Paraskevopoulos, M.K., Christofilos, D., Andrieux, P., Panayiotou, C., 2011. Polymeric hydrogels and supercritical fluids: the mechanism of
406 hydrogel foaming. Polymer 52, 2819-2826.

407 Ulker, Z., Erkey, C., 2014. An emerging platform for drug delivery: aerogel based systems. J. Contr. Release 177, 51-63.

408 Uzer, S., Akman, U., Hortacsu, O., 2006. Polymers welling andi mpregnation using supercritical CO2: a model-component study towards producing
409 controlledrelease drugs. J. Supercrit. Fluids 38, 119-128.

410 Wagh, P.B., Begag, R., Pajonk, G.M., Rao, A.V., Haranath, D., 1999. Comparison of some physical properties of silica aerogel monoliths synthesized by
411 different precursors. Mater. Chem. Phys. 57, 214-218.

412 Watzke, H.J., Dieschbourg, C., 1994. Novel silica-biopolymer nanocomposites: the silica sol-gel process in biopolymer organogels. Adv. Coll. Interf. Sci. 50, 1-
413 14.

414 Wei, Y., Dong, H., Xu, J., Wang, C., Feng, Q., Qiu, K.-Y., Li, Z.-C., Jansen, S.A., 2004. Nonsurfactant route to nanoporous phenyl-modified hybrid silica
415 materials. Nanop. Mater.: Sci. Eng. 188-205.

416 Yasuji, T., Takeuchi, H., Kawashima, Y., 2008. Particle design of poorly water-soluble drug substances using supercritical fluid technologies. Adv. Drug Deliv.
417 Rev. 60, 388-398.

418 Yoda, S., Ohshima, S., 1999. Supercritical drying media modification for silica aerogel preparation. J. Non-Cryst. Solids 248, 224-234.

419 Figure Captions

420 Figure 1. Schematic representation of the molecular structure of the used: (a) aerogel modifiers, and (b) drugs.

421 Figure 2. Selected examples of thermogravimetric profiles recorded for: (a) hydrophilic aerogels with two different gelatin percentages (Table 2), and (b)

422 hydrophobized H3 aerogels involving Ph, C16 or (CH3)3 silyl moiety.

423 Figure 3. SEM images of sample H20 at (a) low, and (b) high magnification.

Figure 4. Solid characterization of hybrid H3 aerogels loaded with the three studied drugs: (a) TGA profiles, and (b) XRD patterns.

Figure 5. Influence on drug loading (HPLC calculated, Table 2) of aerogel composition: (a) gelatin ratio, percentage of (b) -Ph or (c) -C16 additive added to H3, and (d) silylaltion of H3-H30 samples.

Figure 6. Crystalline drugs dissolution profiles at gastric (pH 2.0) and intestinal (pH 6.7) pH-condition: (a) ibuprofen, (b) ketoprofen, and (c) triflusal.

Figure 7. Release behavior from drug@H3 systems for: (a) ibuprofen at pH 2 and 6.7, (b) ketoprofen at pH 2 and 6.7, (c) triflusal at pH 6.7, and (d) triflusal at pH 2.

Figure 8. Contrasted drug release profiles from drug@H3 and drug@H3_sil systems for: (a) ibuprofen at pH 6.7 and 2, (b) ketoprofen at pH 6.7 and 2, (c) triflusal at pH 6.7, and (d) triflusal at pH 2.

438

439

440

441 Table 1 Composition of the precursor mixture for each synthesized aerogel. Data is expressed in grams [g].

Sample	TMOS	MeOH	H_2O	$(NH_4)_2CO_3$	Gelatin	Ph-TMOS	C_{16}-TMOS	HMDS
H3	3.10	5.55	20	0.07	0.10	-	-	-
H10	3.10	5.55	20	0.07	0.30	-	-	-
H20	3.10	5.55	20	0.07	0.60	-	-	-
H30	3.10	5.55	20	0.07	1.00	-	-	-
H3_Ph10	2.79	13.5	10	0.10	0.10	0.32	-	-
H3_Ph20	2.48	13.5	10	0.10	0.10	0.64	-	-
H3_Ph30	2.17	13.5	10	0.10	0.10	0.96	-	-
H3_C_{16}10	2.79	13.5	10	0.10	0.10	-	0.27	-
H3_C_{16}20	2.48	13.5	10	0.10	0.10	-	0.53	-

Sample	TMOS	MeOH	H_2O	$(NH_4)_2CO_3$	Gelatin	Ph-TMOS	C_{16}-TMOS	HMDS
H3_C_{16}30	2.17	13.5	10	0.10	0.10	-	0.80	-
H3_Sil	3.10	5.55	20	0.07	0.10	-	-	2.31
H10_Sil	3.10	5.55	20	0.07	0.30	-	-	2.31
H20_Sil	3.10	5.55	20	0.07	0.60	-	-	2.31
H30_Sil	3.10	5.55	20	0.07	1.00	-	-	2.31

442 Table 2. Composition and textural properties of the precipitated aerogel samples, and HPLC measured drug loading values.

Sample	Gelatin (wt%)	Ph (wt%)	C_{16} (wt%)	$(CH_3)_3$ (wt%)	Sr (molecnm^{-2})	a_s (m^2g^{-1})	C	Ibu (wt%)	Ket (wt%)	Trf(T) (wt%)
H3	3.7	0	0	0	0	704	80	24	14	29
H10	11	0	0	0	0	527	83	23	14	25
H20	18	0	0	0	0	390	78	22	15	29
H30	24	0	0	0	0	303	70	19	11	29
H3_Ph10	5.0	4.2	0	0	0.49	-	-	23	18	27
H3_Ph20	3.8	7.6	0	0	0.84	762	55	19	13	29
H3_Ph30	4.0	9.2	0	0	1.02	-	-	18	9.1	27
H3_C_{16}10	~ 4[a]	0	2.1	0	0.08	-	-	27	11	24

Sample	Gelatin (wt%)	Ph (wt%)	C_{16} (wt%)	$(CH_3)_3$ (wt%)	Sr (molecnm^{-2})	a_s (m^2g^{-1})	C	Ibu (wt%)	Ket (wt%)	Trf(T) (wt%)
H3_C1620	~ 4[a]	0	4	0	0.17	710	73	25	7.2	21
H3_C1630	~ 4[a]	0	5.8	0	0.24	-	-	25	11	19
H3_sil	3.6	0	0	6.1	1.16	650	22	15	7.0	18
H10_sil	-	-	-	-	-	-	-	14	7.7	22
H20_sil	19	0	0	5	1.71	-	-	16	9.1	25
H30_sil	24	0	0	6.5	1.05	-	-	15	8.4	26

(a)

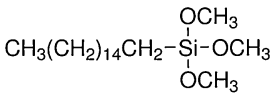

C_{16}-TMOS

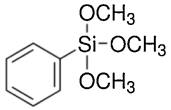

Ph-TMOS

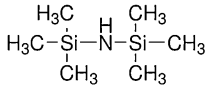

HMDS

(b)

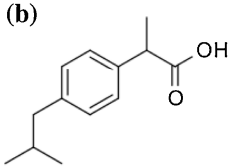

Ibu

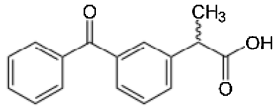

Ket

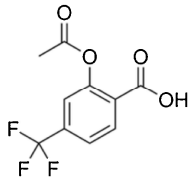

Trf

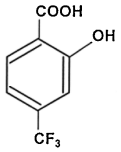

HTB

Fig 1

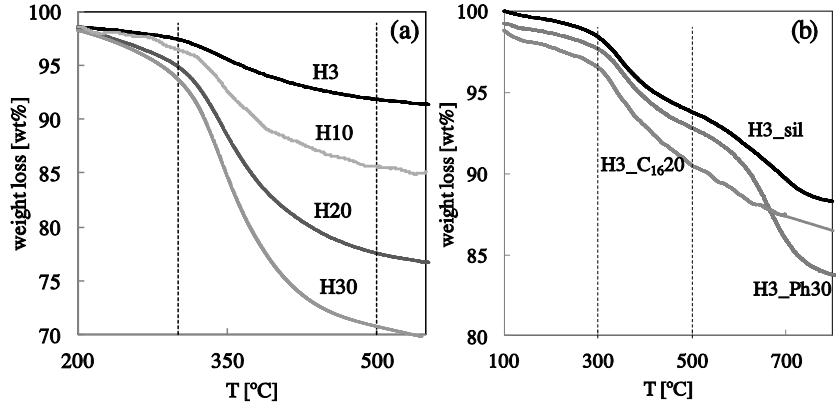

Fig 2

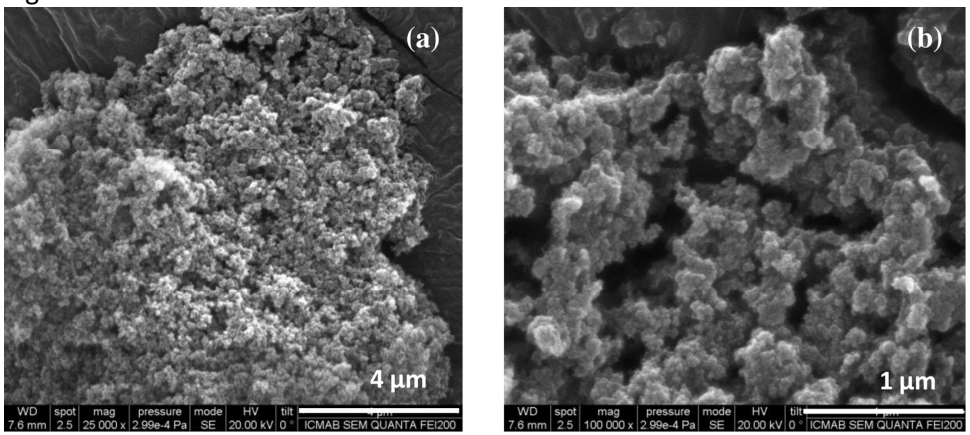

Fig 3

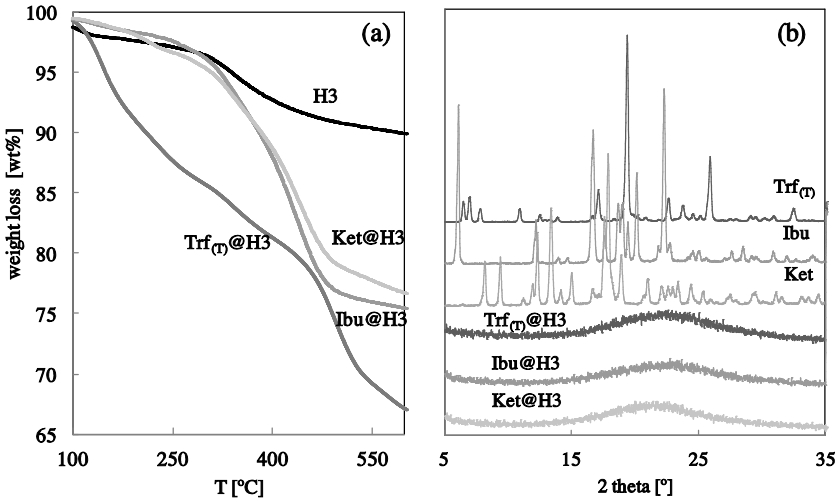

452
453 Fig 4

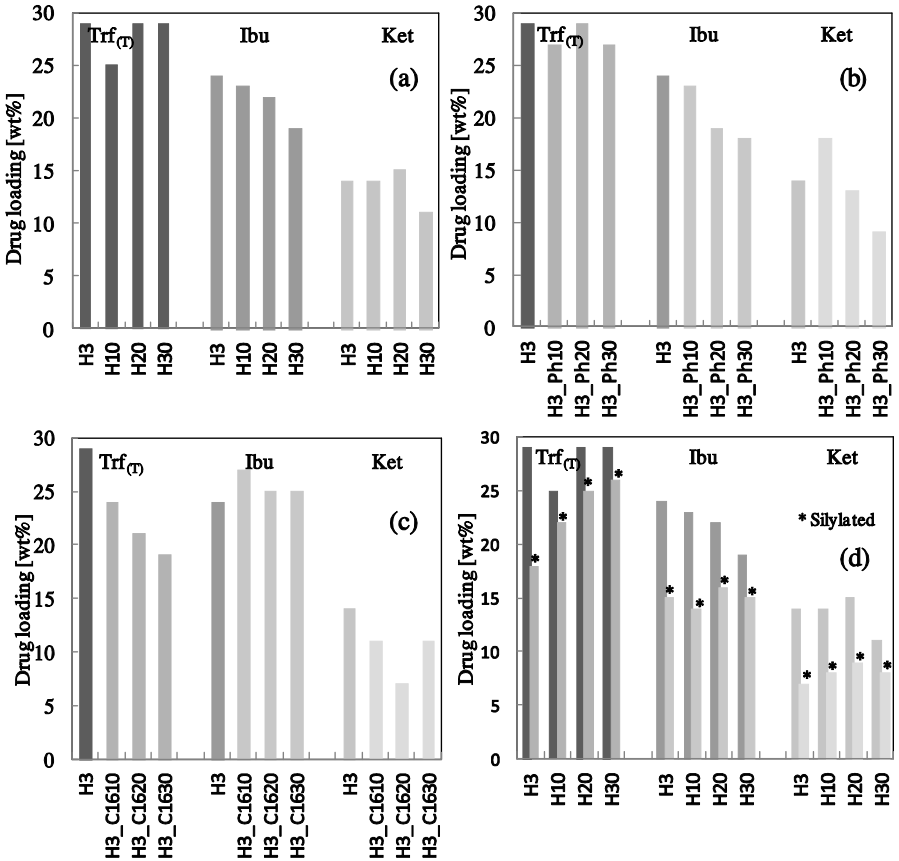

454
455 Fig 5

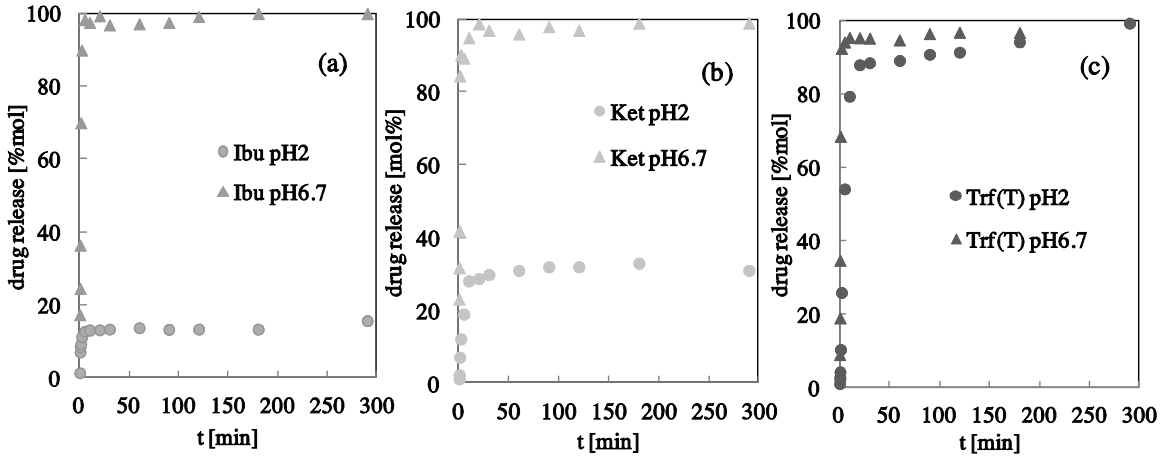

Fig 6

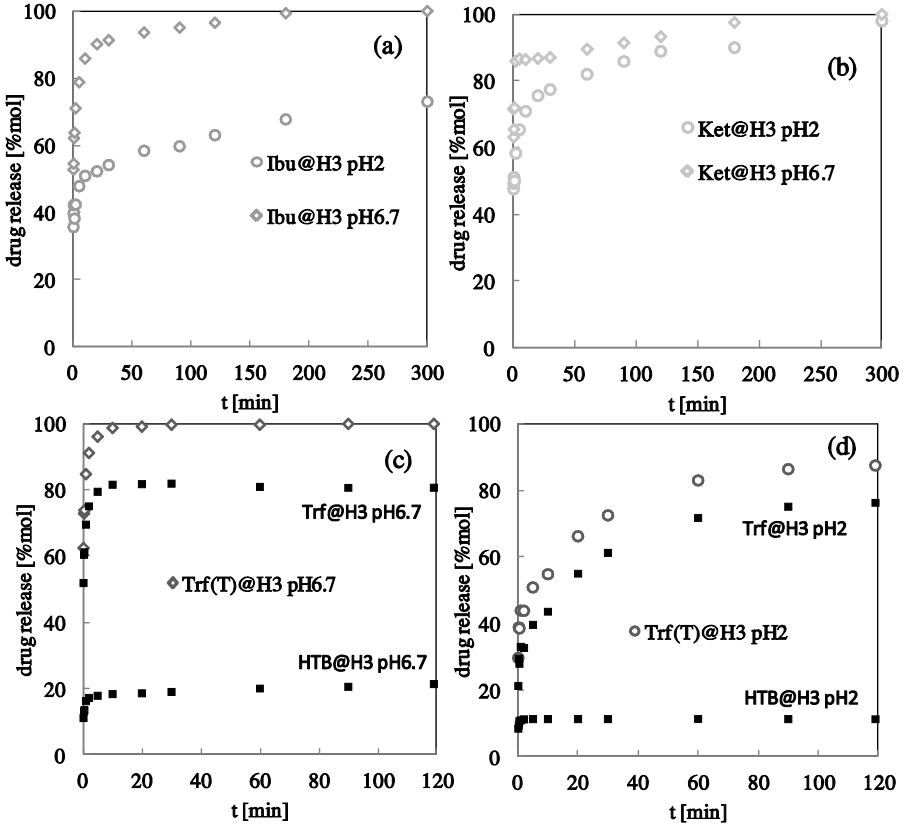

458
459 Fig 7

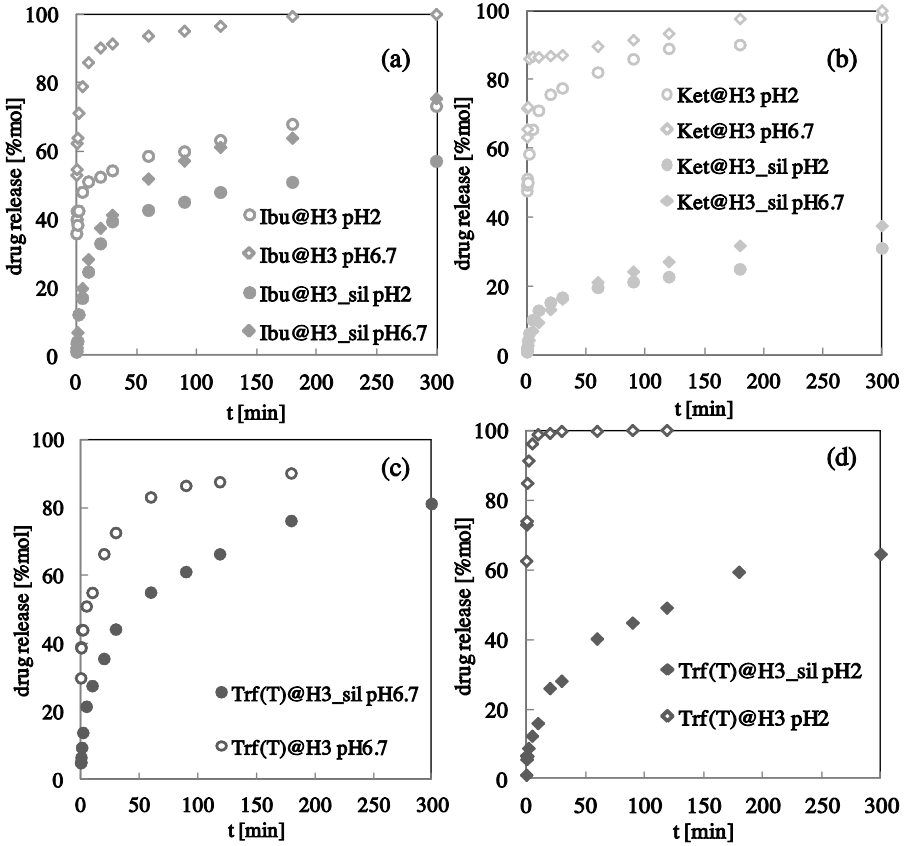

460
461 Fig 8